Fabrication of TiO 2 Nanotanks Embedded in a Nanoporous Alumina Template

Christophe Massard, S. Pairis, V. Raspal, Y. Sibaud, K. Awitor

Hindawi Publishing Corporation
Journal of Nanomaterials
Volume 2015, Article ID 452148, 7 pages
http://dx.doi.org/10.1155/2015/452148

Research Article

Fabrication of TiO_2 Nanotanks Embedded in a Nanoporous Alumina Template

C. Massard,[1] S. Pairis,[2] V. Raspal,[1] Y. Sibaud,[1] and K. O. Awitor[1]

[1]*Clermont Université, Université d'Auvergne, C-Biosenss EA 4676, BP 10448, 63000 Clermont-Ferrand, France*
[2]*Institut NEEL, CNRS, Université Grenoble Alpes, BP 166, 38042 Grenoble Cedex 9, France*

Correspondence should be addressed to C. Massard; christophe.massard@udamail.fr

Received 12 March 2015; Revised 18 May 2015; Accepted 24 May 2015

Academic Editor: Xiaosheng Fang

The feasibility of surface nanopatterning with TiO_2 nanotanks embedded in a nanoporous alumina template was investigated. Self-assembled anodized aluminium oxide (AAO) template, in conjunction with sol gel process, was used to fabricate this nanocomposite object. Through hydrolysis and condensation of the titanium alkoxide, an inorganic TiO_2 gel was moulded within the nanopore cavities of the alumina template. The nanocomposite object underwent two thermal treatments to stabilize and crystallize the TiO_2. The morphology of the nanocomposite object was characterized by Field Emission Scanning Electron Microscopy (FESEM). The TiO_2 nanotanks obtained have cylindrical shapes and are approximately 69 nm in diameter with a tank-to-tank distance of 26 nm. X-ray diffraction analyses performed by Transmission Electron Microscopy (TEM) with selected area electron diffraction (SAED) were used to investigate the TiO_2 structure. The optical properties were studied using UV-Vis spectroscopy.

1. Introduction

Nanostructured surfaces with the possible management of behavioral characteristics of the solid-liquid interface as well as their enormous surface area are critical in fields such as environment, health, electronics, IT, and energy. So, nanostructures are required to develop emerging technologies such as miniaturization of functional devices [1, 2] or to design more efficient materials [3–5]. The ability to produce nanostructures also allows developing devices [6, 7] that rely on physical principles that are missing at the microscopic scale such as quantum size effect. In some of emerging technological applications, such as nanomedicine, fabricating the nanostructures is a great challenge and the key event to the achievement of the desired applications. Numerous techniques are nowadays available to build the nanostructures such as printing [8], molding [9], embossing [10], or anodic oxidation [11]. Hollow shaped nanostructures provide a platform to develop biomedical applications [12–14] and to store chemicals in nanocages [15–17]. In nanomedicine, nanocavities can be useful to encapsulate therapeutic agents in order to create drug delivery devices with controlled-release properties [18, 19]. Many methods are available to fabricate TiO_2 nanotubes. The most commonly used are the electrochemical deposition methods [20], atomic layer deposition [21] and template assisted deposition [22]. Electrochemical anodizations of titanium sheet are simple, cost effective methods. However, the obtained TiO_2 nanotubes layers are generally not very ordered compared to AAO (anodic aluminum oxide) obtained by electrochemical anodization.

The hydro/solvothermal methods with or without templates enable excellent control over the nanotube dimensions, including their wall thickness, diameter, and height. These approaches require a control of many parameters (solvent, annealing temperature) to be efficient. The atomic layer deposition requires more costly instruments. In this work, we demonstrate the feasibility of surface nanopatterning with TiO_2 nanotanks embedded in a nanoporous template by combined electrochemical anodization and sol gel process. This approach is most cost effective, scalable (by changing the AAO nanomould size), and faster. The anodized aluminum oxide (AAO) templates elaborated in this study were used as

nanomoulds whereas the casting of an inorganic sol in the nanopores leads to the TiO_2 nanotanks buildings via a sol gel process after stripping apart the alumina nanomould. Our method ensures that our nanotanks are embedded in AAO templates which give the structure a more rigid base compared to anodized samples. In addition, the TiO_2 sublayer strengthens the barrier layer.

2. Experimental Section

2.1. AAO Templates Synthesis. AAO templates were fabricated using a two-step anodization process on a pure (99.999%) Al foil described in detail elsewhere [23–25]. First, the Al foil was anodized in 0.3 M oxalic acid solution at 40 V and 3°C for 15 h to grow a thick porous oxide layer. The resulting AAO film was then chemically stripped from the Al foil and a secondary anodization in the same oxalic acid solution at 40 V and 3°C for 10 min was carried out. As-grown pore radii can be increased by chemical etching, without a noticeable change in the film thickness. This pore widening is linear in time with the diameters increasing about 6.6 nm per hour. Using this two-step technique combined with the etching process, good ordering is obtained over micron-sized regions and results in an AAO film approximately 400 nm in thickness with 50 nm pore diameters spaced 100 nm apart. A through-hole mask was prepared by separating the AAO film from the Al foil in a saturated $HgCl_2$ solution and removing the bottom alumina barrier layer in 5 wt.% phosphoric acid at 30°C for 34 min. The remaining AAO was then lifted off onto the prepared wet TiO_2 gel layer supported on various substrates.

2.2. Sol Preparation. The synthetic route of the sol chosen here offered a simple method for the preparation of a sol suitable for the deposition of thin film by dip coating process. The sol was based on the dilution of the titanium (IV) butoxide $Ti(OBu)_4$ (3% molar) in anhydrous ethyl alcohol (97% molar), both supplied by Sigma Aldrich. The molar ratio was defined in order to obtain a suitable quality of titanium oxide [26].

2.3. Coating Procedure and Template Assembly. We prepared TiO_2 film coatings on various substrates, such as non-alkali glass plates, silicon wafers, and titanium foils, respectively, for XRD, UV-Vis, and SEM characterization. Every substrate was cleaned and degreased by immersion in 4 ultrasonic baths for 5 minutes containing, respectively, trichloroethylene, acetone, methyl alcohol, and deionized water. Samples were blow-dried under nitrogen flow. Just before the coating, the substrates were cleaned with optical paper and ethyl alcohol. Figure 1 shows the schematic procedure for preparation of TiO_2 nanotanks embedded in a nanoporous alumina template. The starting point is a titanium foil. A thin layer of TiO_2 is deposited by dip coating. The AAO template with both sides opened is then lifted to the wet inorganic TiO_2 coating (Figure 1(a)). The AAO nanocavities are filled with the titanium alkoxide sol (Figure 1(b)). The sol in excess at the surface is wiped using optical paper (Figure 1(c)). The assembly is then heat-treated in order to densify the relief and to crystallize the titanium oxide. A development step is then applied in order to partially remove AAO template (Figure 1(d)). We obtained TiO_2 nanotanks embedded in a nanoporous template (Figure 1(e)).

2.4. Annealing Treatment. After 20 minutes of air drying at room temperature, the samples were first heat-treated in an oven at 130°C for one hour under air. This first curing step allowed stabilizing the titanium oxide layer and also removing volatile organic solvent. The second part of the annealing took place in a tubular furnace at 500°C for one hour under air in order to obtain crystallized titanium dioxide material. A crystallized material was found to be less sensitive to the chemical stripping reagents used to remove partially the alumina nanomould than the amorphous counterpart.

2.5. Scanning Electron Microscopy. The samples were characterized by a Field Emission Scanning Electron Microscope (FESEM) from ZEISS ultra+ (ZEISS-Germany) used with a low voltage (900 V and 3 kV) to limit charge effects. The working distance was from 2.5 mm to 6 mm. Samples were observed on a flat view or with a various tilt angle (33° and 40°). Pictures were obtained with the secondary electron detector in-lens. Theses characterizations were carried on at the Neel Institute of Grenoble.

2.6. Transmission Electron Microscope and X-Ray Microanalysis. For detailed analysis of the nanotanks, a CM300 Philips Transmission Electron Microscope (TEM) equipped with an X-ray microanalysis system by energy dispersion (Bruker EDX system SDD X-Flash 5030 detector) was used. The energy of the electrons is 300 KeV, leading to a wavelength of about 0.0196 Å. Images and electron diffraction patterns are obtained in selected area on aggregate with a TVIPS-F416 camera (4 k × 4 k 16 bits). Samples were prepared by scratching the surface which was rinsed with ethanol. The ethanol solution with nanoobjects was filtered using a 3 mm copper TEM grid covered with an amorphous carbon membrane with holes.

2.7. XRD Analysis. The crystalline structure of the TiO_2 layers was determined by XRD using a Philips X'pert Pro diffractometer with Cu Kα radiation.

2.8. UV-Vis Spectroscopy. Transmission spectra of the samples coated on silicon were recorded from 200 to 900 nm with a resolution of 2 nm using a Perkin Elmer Lambda 35 spectrometer.

3. Results and Discussion

3.1. AAO Templates as Nanomould. Figure 2(a) shows a top-down SEM image of a typical nanoporous alumina template. This image indicates pore regularity with good hexagonal order. The resulting sample is roughly 10 mm × 10 mm in size, presenting a good uniformity. Figure 2(b) shows an oblique angle view from which the template thickness H was measured (H = 500 nm in this case). Considering the good regularity of the synthesized nanoporous structure previously

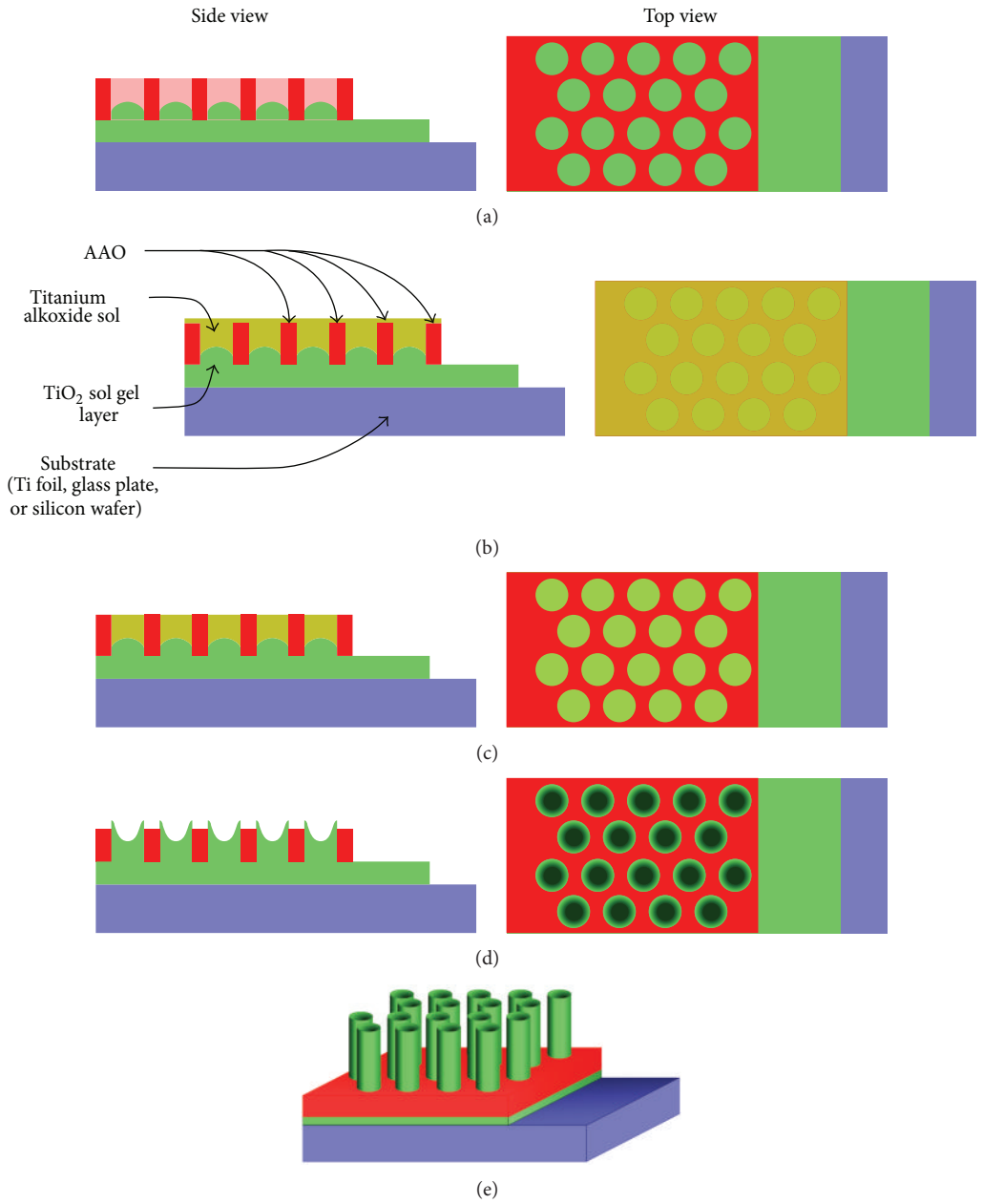

Figure 1: Schematic procedure for preparation of TiO_2 nanotanks embedded in a nanoporous alumina template: (a) the AAO template with both sides opened is lifted to the wet inorganic TiO_2 coating. (b) The AAO nanocavities are filled with the titanium alkoxide sol. (c) The sol in excess at the surface is wiped. (d) After the annealing, a development step is then applied in order to remove partially AAO template. (e) TiO_2 nanotanks embedded in an AAO nanoporous template are obtained.

depicted, the AAO template was a good candidate to be used as a nanomould for building the TiO_2 nanotanks.

Figure 3 shows FESEM micrographs of the TiO_2 nanotanks embedded in AAO template as described in Figure 1. Figure 3(a) shows the whole assembly. Figure 3(b) shows the top-down images of the hexagonal arrangement of the nanotanks resulting from the hexagonal pore structure in the AAO template. The ordered TiO_2 nanotanks are approximately 69 nm in diameter with a tank-to-tank separation of 26 nm. The SEM pictures of as-grown AAO in Figure 2 show the AAO template with 50 nm diameter. A free-standing through-hole membrane may then be obtained by getting rid of the bottom barrier layer. This was achieved by chemical dissolution. The layer turns into a permeable membrane. This process increases the pore radii of the through-hole AAO template. So the diameter of nanotanks is around 69 nm in agreement with the through-hole AAO template diameter. Figure 3(c) shows a 33° oblique angle FESEM view of the TiO_2 nanotanks. This picture shows fallen nanotanks occurring during the AAO unmolding process. The approximate height

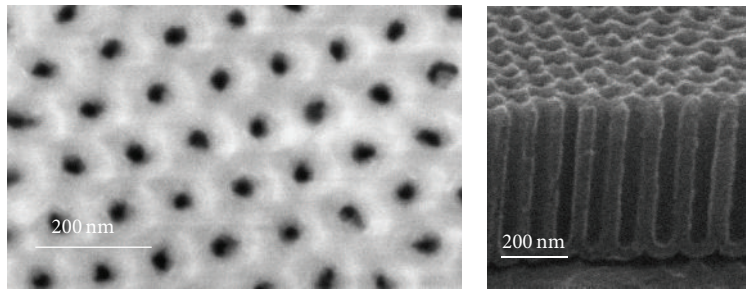

(a) (b)

Figure 2: Secondary electron (FESEM) images obtained with the secondary electron detector, in-lens, of a nanoporous alumina template: (a) top view and (b) oblique view.

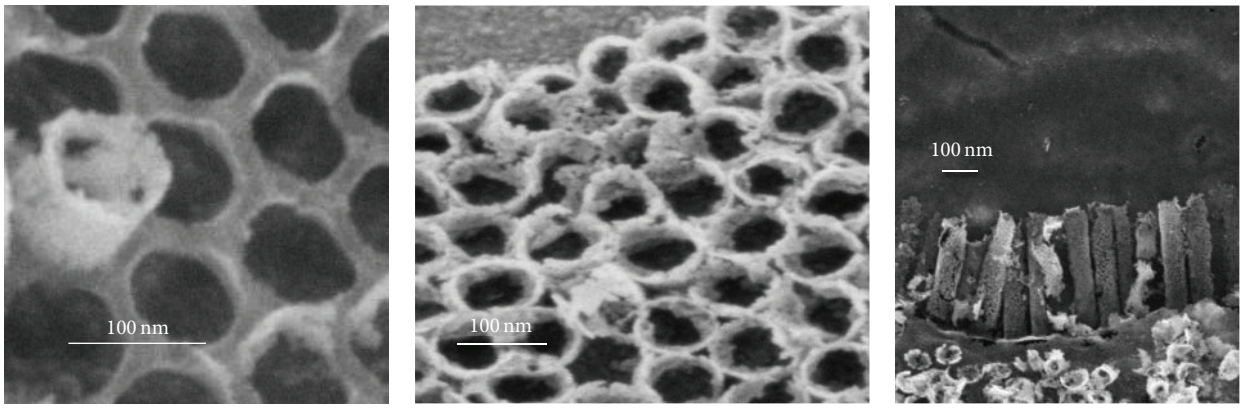

(a) (b) (c)

Figure 3: FESEM (secondary electron collected with the in-lens detector) micrographs of the TiO_2 nanotanks embedded in AAO template. (a) TiO_2 nanotanks embedded in AAO template. (b) Image of the hexagonal arrangement of the nanotanks. (c) View of the fallen TiO_2 nanotanks.

determined from the image showing fallen nanotanks was found to be 440 nm. From these images, it can be seen that the TiO_2 nanotanks have cylindrical shapes with porous surface.

3.2. Transmission Electron Microscope and X-Ray Microanalysis. A TEM image of a TiO_2 nanotank is presented in Figure 4. The nanotank appears as a stack of spherical-like grains crammed together. These kinds of elementary grains are roughly 90 nm thick in diameter. Because of this granular morphology, the nanotank's surface exhibits a rough and porous surface. EDX-MET spectrum is presented in Figure 5. The major peaks match with titanium and oxygen species and are relative to the elaborated titanium dioxide nanotanks. Copper peaks come from the copper grid used as specimen holder. Sometimes aluminum, phosphor, and silicon traces are detected. Theses traces are the result of the different chemicals used in the synthesis protocol. The crystallinity of the TiO_2 nanotanks structures are determined by indexing the diffraction pattern obtained (see Figure 6). Rings on the diffraction patterns are indexed by anatase phase I41/amd (S.G.: 141; a = 3,7852 Å, c = 9,514 Å; pattern 00-021-1272) (labels are reported on it). The experimental data are in good agreement with the standard 021-1272 concerning anatase.

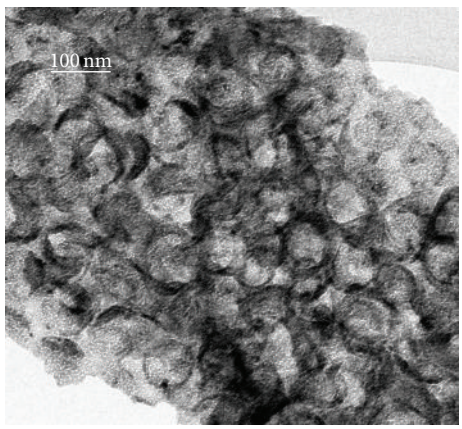

Figure 4: TEM image of the TiO_2 nanotank surface.

3.3. XRD Analysis. Figure 7 summarizes the X-ray characterization of TiO_2 layers on quartz substrate before and after annealing at 500°C in air for 2 h. The unannealed TiO_2 layer is amorphous. In order to convert the TiO_2 layer to a crystalline phase, the sample was annealed in air at 500°C in increments

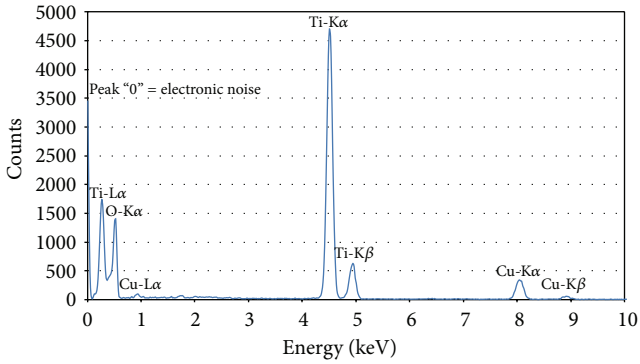

Figure 5: MET-EDX spectra of the TiO_2 nanotanks.

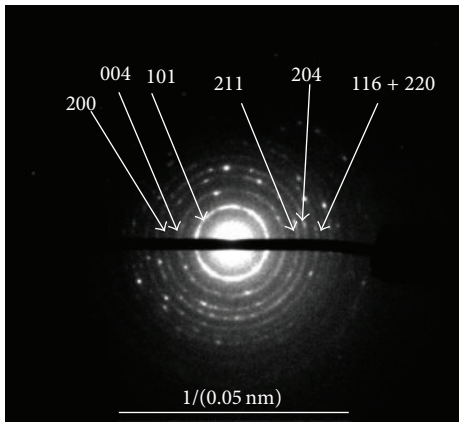

Figure 6: Diffraction pattern of the TiO_2 nanotanks.

of 50°C. We observe the characteristic line of anatase (1 0 1). Crystallite size was calculated using the Scherrer formula

$$D = \frac{0.94\lambda}{\beta \cos\theta}, \quad (1)$$

where λ is the wavelength of the CuKα_1 line, θ is the Bragg diffraction angle, and β is the full-width at half-max (FWHM) of a peak. We calculated the crystallite size by using the FWHM of the anatase (1 0 1). The average crystal size is about 64 nm. These data are in the same order of magnitude with the crystallite size evaluated from the TEM images.

3.4. UV-Vis Spectroscopy. Figure 8 plots the UV-Vis absorbance spectra for quartz substrate alone and quartz substrate coated with thin film layer stabilized at 130°C for 1 hour. The curve for TiO_2 thin film layer shows considerable absorption for wavelengths below 330 nm which is in good agreement with previous studies [27].

A deviation of band gap energy is obtained on the nanotank titanium dioxides. This is a consequence of the weak thickness of our nanostructured layer. This result was observed elsewhere [28].

3.5. Discussion. We have obtained TiO_2 nanotanks using AAO template as nanomould. The approach followed here enables the fabrication of nanocylinders arrays at the surface

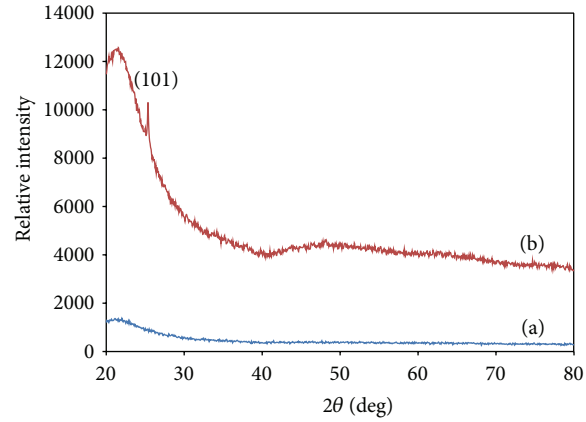

Figure 7: X-ray diffraction patterns of TiO_2 layers on quartz substrate: (a) as grown, (b) annealed at 500°C.

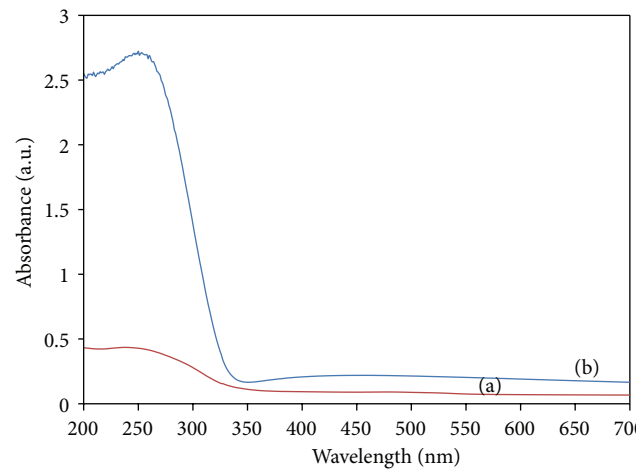

Figure 8: UV-Vis spectra for (a) quartz substrate coated with TiO_2 thin film layer, (b) quartz substrate alone layer (reference).

of an inorganic coating. TEM images exhibit hollow shaped structures. The titanium alkoxide sol used to fill in the AAO template is responsible for establishing theses cavities. During the annealing step, a TiO_2 gel is formed within the AAO templates. Considering the high amount of volatile organic compound in the sol, evaporation during the heat treatment is responsible for the cavities genesis in the nanocylinders. After a development step, the AAO template is partially removed in order to exhibit the so-called nanotanks consisting in TiO_2 hollow nanocylinders ruffling a base alumina. In comparison with conventional TiO_2 nanotubes layers obtained by electrochemical anodization, we highlighted a more regular shape of the TiO_2 nanotanks as a consequence of the growing of the TiO_2 nanotanks into cylindrical AAO nanomoulds (see Figure 9). This geometrical improvement of the shape is an advantage of the combined electrochemical anodization and sol gel process.

These hollow nanostructures are interesting in building future drug delivery platform. In previous works, we have

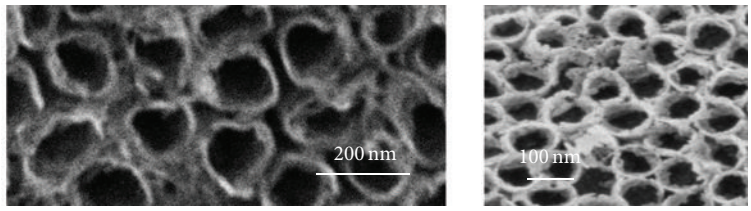

(a) (b)

Figure 9: FESEM (secondary electron collected with the in-lens detector) micrographs of the TiO_2 comparison: (a) image of conventional TiO_2 nanotubes layers obtained by electrochemical anodization [11], (b) TiO_2 nanotanks embedded in AAO template.

demonstrated that TiO_2 nanotubes obtained by electrochemical anodization could act as cefuroxime carriers [29]. During the same annealing treatment, a crystallization process of the TiO_2 inorganic backbone occurs, providing an anatase structure to the synthesized nanotank relief. Our surface nanostructuration, combining electrochemical process and sol gel route, can also be a photoactive device to inhibit bacterial adhesion [30–34].

4. Conclusion

We demonstrate the feasibility of surface nanopatterning with TiO_2 nanotanks embedded in a nanoporous template by combined electrochemical anodization and sol gel process. The ordered crystallized TiO_2 nanotanks obtained have cylindrical shape and are approximately 69 nm in diameter with a tank-to-tank separation of 26 nm.

The nanotanks obtained are promising candidates for further applications concerning nanoconfinement and drug administration: the embedded TiO_2 nanotanks are a stiff and protective nanocage which can be used to store and protect different molecular species of interest.

Furthermore, the anatase structure of the TiO_2 material exhibits photocatalytic properties. If required, an UV irradiation of the nanostructure can provide a bactericidal effect: each cavity can own a self-cleaning surface, without the use of disinfection chemical products that might interfere with the stored molecules.

So our new synthesis method is a contribution to the building of well defined TiO_2 nanotanks with a cylindrical geometry. The geometrical uniformity of our TiO_2 nanotanks is a consequence of the use of nanoporous alumina template as nanomoulds.

The growing of TiO_2 nanotanks in AAO template by combining anodization technique and sol gel process ensures a better geometrical definition of the TiO_2 nanotanks obtained compared to classical anodization of titanium. Monodisperse hollow nanocylinders consisting of crystalline titania particles have been already prepared in a porous alumina membrane by a deposition technique using an aqueous solution system of titanium tetrafluoride. The main difference with our approach is the previous deposition of a titanium oxide gel layer. This film ensures a better anchoring for the coming TiO_2 nanotanks, in order to obtain arrays of TiO_2 nanotanks with a preferential orientation.

Conflict of Interests

The authors declare that there is no conflict of interests regarding the publication of this paper.

Acknowledgments

The authors thank Joel Cellier for the XRD measurements and the Neel Institute of Grenoble for FESEM and TEM microscopies and X-ray microanalysis.

References

[1] A. Martínez-Otero, E. Evangelio, R. Alibés et al., "Surface-structured molecular sensor for the optical detection of acidity," *Langmuir*, vol. 24, no. 7, pp. 2963–2966, 2008.

[2] P. Hu, J. Zhang, L. Li, Z. Wang, W. O'Neill, and P. Estrela, "Carbon nanostructure-based field-effect transistors for label-free chemical/biological sensors," *Sensors*, vol. 10, no. 5, pp. 5133–5159, 2010.

[3] Y.-G. Guo, Y.-S. Hu, W. Sigle, and J. Maier, "Superior electrode performance of nanostructured mesoporous TiO_2 (Anatase) through efficient hierarchical mixed conducting networks," *Advanced Materials*, vol. 19, no. 16, pp. 2087–2091, 2007.

[4] Y. Jin, Y. Shen, and S. Dong, "Electrochemical design of ultrathin platinum-coated gold nanoparticle monolayer films as a novel nanostructured electrocatalyst for oxygen reduction," *Journal of Physical Chemistry B*, vol. 108, no. 24, pp. 8142–8147, 2004.

[5] S. Zhang, D. M. Marini, W. Hwang, and S. Santoso, "Design of nanostructured biological materials through self-assembly of peptides and proteins," *Current Opinion in Chemical Biology*, vol. 6, no. 6, pp. 865–871, 2002.

[6] P. Caroff, C. Paranthoen, C. Platz et al., "High-gain and low-threshold InAs quantum-dot lasers on InP," *Applied Physics Letters*, vol. 87, Article ID 243107, 2005.

[7] H.-J. Choi, J. C. Johnson, R. He et al., "Self-organized GaN quantum wire UV lasers," *The Journal of Physical Chemistry B*, vol. 107, no. 34, pp. 8721–8725, 2003.

[8] L. Jiao, B. Fan, X. Xian, Z. Wu, J. Zhang, and Z. Liu, "Creation of nanostructures with poly(methyl methacrylate)-mediated nanotransfer printing," *Journal of the American Chemical Society*, vol. 130, no. 38, pp. 12612–12613, 2008.

[9] H. Xu, N. Lu, D. Qi et al., "Biomimetic antireflective Si nanopillar arrays," *Small*, vol. 4, no. 11, pp. 1972–1975, 2008.

[10] Z.-K. Shen, Z.-H. Chen, Z.-J. Qiu et al., "Influences of embossing technology on $Pb(Zr_{0.3},Ti_{0.7})O_3$ ferroelectric thin film," *Microelectronic Engineering*, vol. 87, no. 5–8, pp. 869–871, 2010.

[11] K. O. Awitor, S. Rafqah, G. Géranton et al., "Photo-catalysis using titanium dioxide nanotube layers," *Journal of Photochemistry and Photobiology A: Chemistry*, vol. 199, no. 2-3, pp. 250–254, 2008.

[12] S. E. Skrabalak, J. Chen, L. Au, X. Lu, X. Li, and Y. Xia, "Gold nanocages for biomedical applications," *Advanced Materials*, vol. 19, no. 20, pp. 3177–3184, 2007.

[13] K. K. Perkin, J. L. Turner, K. L. Wooley, and S. Mann, "Fabrication of hybrid nanocapsules by calcium phosphate mineralization of shell cross-linked polymer micelles and nanocages," *Nano Letters*, vol. 5, no. 7, pp. 1457–1461, 2005.

[14] A. Vinu, M. Miyahara, V. Sivamurugan, T. Mori, and K. Ariga, "Large pore cage type mesoporous carbon, carbon nanocage: a superior adsorbent for biomaterials," *Journal of Materials Chemistry*, vol. 15, no. 48, pp. 5122–5127, 2005.

[15] O. V. Pupysheva, A. A. Farajian, and B. I. Yakobson, "Fullerene nanocage capacity for hydrogen storage," *Nano Letters*, vol. 8, no. 3, pp. 767–774, 2008.

[16] Z. Wang and X. W. Lou, "TiO_2 nanocages: fast synthesis, interior functionalization and improved lithium storage properties," *Advanced Materials*, vol. 24, no. 30, pp. 4124–4129, 2012.

[17] T. Oku, M. Kuno, and I. Narita, "Hydrogen storage in boron nitride nanomaterials studied by TG/DTA and cluster calculation," *Journal of Physics and Chemistry of Solids*, vol. 65, no. 2-3, pp. 549–552, 2004.

[18] C. Pinto Reis, R. J. Neufeld, A. J. Ribeiro, and F. Veiga, "Nanoencapsulation I. Methods for preparation of drug-loaded polymeric nanoparticles," *Nanomedicine: Nanotechnology, Biology, and Medicine*, vol. 2, no. 1, pp. 8–21, 2006.

[19] A. Kumari, S. K. Yadav, and S. C. Yadav, "Biodegradable polymeric nanoparticles based drug delivery systems," *Colloids and Surfaces B: Biointerfaces*, vol. 75, no. 1, pp. 1–18, 2010.

[20] P. Roy, S. Berger, and P. Schmuki, "TiO_2 nanotubes: synthesis and applications," *Angewandte Chemie International Edition*, vol. 50, no. 13, pp. 2904–2939, 2011.

[21] M. S. Sander, M. J. Côté, W. Gu, B. M. Kile, and C. P. Tripp, "Template-assisted fabrication of dense, aligned arrays of titania nanotubes with well-controlled dimensions on substrates," *Advanced Materials*, vol. 16, no. 22, pp. 2052–2057, 2004.

[22] H. Imai, Y. Takei, K. Shimizu, M. Matsuda, and H. Hirashima, "Direct preparation of anatase TiO_2 nanotubes in porous alumina membranes," *Journal of Materials Chemistry*, vol. 9, no. 12, pp. 2971–2972, 1999.

[23] H. Masuda and K. Fukuda, "Ordered metal nanohole arrays made by a two-step replication of honeycomb structures of anodic alumina," *Science*, vol. 268, no. 5216, pp. 1466–1468, 1995.

[24] A.-P. Li, A. F. Muller, A. Birner, K. Nielsch, and U. Gösele, "Hexagonal pore arrays with a 50–420 nm interpore distance formed by self-organization in anodic alumina," *Journal of Applied Physics*, vol. 84, no. 11, pp. 6023–6026, 1998.

[25] O. Jessensky, F. Müller, and U. Gösele, "Self-organized formation of hexagonal pore structures in anodic alumina," *Journal of the Electrochemical Society*, vol. 145, no. 11, pp. 3735–3740, 1998.

[26] B. Samuneva, V. Kozhukharov, C. Trapalis, and R. Kranold, "Sol-gel processing of titanium-containing thin coatings—part I Preparation and structure," *Journal of Materials Science*, vol. 28, no. 9, pp. 2353–2360, 1993.

[27] J. Zhang, M. Li, Z. Feng, J. Chen, and C. Li, "UV Raman spectroscopic study on TiO_2. I. Phase transformation at the surface and in the bulk," *The Journal of Physical Chemistry B*, vol. 110, no. 2, pp. 927–935, 2006.

[28] K. O. Awitor, A. Rivaton, J.-L. Gardette, A. J. Down, and M. B. Johnson, "Photo-protection and photo-catalytic activity of crystalline anatase titanium dioxide sputter-coated on polymer films," *Thin Solid Films*, vol. 516, no. 8, pp. 2286–2291, 2008.

[29] P. Chennell, E. Feschet-Chassot, T. Devers, K. O. Awitor, S. Descamps, and V. Sautou, "In vitro evaluation of TiO_2 nanotubes as cefuroxime carriers on orthopaedic implants for the prevention of periprosthetic joint infections," *International Journal of Pharmaceutics*, vol. 455, no. 1-2, pp. 298–305, 2013.

[30] V. Antoci Jr., C. S. Adams, J. Parvizi, P. Ducheyne, I. M. Shapiro, and N. J. Hickok, "Covalently attached vancomycin provides a nanoscale antibacterial surface," *Clinical Orthopaedics and Related Research*, no. 461, pp. 81–87, 2007.

[31] N. Mitik-Dineva, J. Wang, R. C. Mocanasu, P. R. Stoddart, R. J. Crawford, and E. P. Ivanova, "Impact of nano-topography on bacterial attachment," *Biotechnology Journal*, vol. 3, no. 4, pp. 536–544, 2008.

[32] D. Campoccia, L. Montanaro, H. Agheli et al., "Study of *Staphylococcus aureus* adhesion a novel nanostructured surface by chemiluminometry," *International Journal of Artificial Organs*, vol. 29, no. 6, pp. 622–629, 2006.

[33] F.-P. Lee, D.-J. Wang, L.-K. Chen et al., "Antibacterial nanostructured composite films for biomedical applications: microstructural characteristics, biocompatibility, and antibacterial mechanisms," *Biofouling*, vol. 29, no. 3, pp. 295–305, 2013.

[34] L. Montanaro, D. Campoccia, and C. R. Arciola, "Nanostructured materials for inhibition of bacterial adhesion in orthopedic implants: a minireview," *International Journal of Artificial Organs*, vol. 31, no. 9, pp. 771–776, 2008.